Energy resolution and dynamical heterogeneity effects on elastic incoherent neutron scattering from molecular systems

Torsten Becker and Jeremy C. Smith*
Computational Molecular Biophysics, Interdisciplinary Center for Computational Science (IWR), Universität Heidelberg, Im Neuenheimer Feld 368, D-69120 Heidelberg, Germany

(Received 3 May 2002; revised manuscript received 23 August 2002; published 18 February 2003)

Incoherent neutron scattering is widely used to probe picosecond-nanosecond time scale dynamics of molecular systems. In systems of spatially confined atoms the relatively high intensity of elastic incoherent neutron scattering is often used to obtain a first estimate of the dynamics present. For many complex systems, however, experimental elastic scattering is difficult to interpret unambiguously using analytical dynamical models that go beyond the determination of an average mean-square displacement. To circumvent this problem a description of the scattering is derived here that encompasses a variety of analytical models in a common framework. The framework describes the time-converged part of the dynamic structure factor [the elastic incoherent scattering function (EISF)] and lends itself to practical use by explicitly incorporating effects due to the finite energy resolution of the instrument used. The dependence of the elastic scattering on wave vector is examined, and it is shown how heterogeneity in the distribution of mean-square displacements can be related to deviations of the scattering from Gaussian behavior. In this case, a correction to fourth order in the scattering vector can be used to extract the variance of the distribution of mean-square displacements. The formalism is used in a discussion of measurements on dynamics accompanying the glass transition in molecular systems. By fitting to experimental data obtained on a protein solution the present methodology is used to show how the existence of a temperature-dependent relaxation frequency can lead to a transition in the measured mean-square displacement in the absence of an EISF change.

DOI: 10.1103/PhysRevE.67.021904 PACS number(s): 87.15.−v, 87.64.Bx

I. INTRODUCTION

Incoherent neutron scattering is a powerful technique for investigating picosecond and nanosecond time scale dynamics of condensed-phase molecular systems [1,2]. The scattering function $S(\vec{Q},\omega)$ (where $\hbar\vec{Q}$ is the momentum change and $\hbar\omega$ the energy change of the scattered neutrons) contains information on both the time scales and the spatial characteristics of the dynamical relaxation processes involved.

The guiding picture in interpreting dynamic neutron scattering is that of a potential energy surface or ''energy landscape.'' The shape of this energy landscape determines the associated microscopic dynamics. For condensed-phase molecular systems the energy landscape can be complex and rugged with many local minima. This leads to the presence of a wide range of vibrational and diffusive dynamical processes. This complexity, together with instrumental limitations in the accessible $(\vec{Q},\omega)$ space, can make unequivocal interpretation of experimental data using simplified, analytical descriptions of the dynamics (such as jump models or continuous diffusion) difficult. One manifestation of this difficulty is the array of analytical descriptions which have been proposed to model the experimental finding that many condensed-phase molecular systems undergo a deviation from harmonic, linear dependence of the average atomic mean-square displacement $\langle\Delta r^2\rangle$ with increasing temperature ($\langle\Delta r^2\rangle$ is accessible via the $Q\rightarrow 0$ behavior of the elastic incoherent scattering). Systems for which such a ''dynamical transition'' has been observed include glass-forming liquids, polymers, and proteins [3–9]. For proteins, suggestions have been made that the additional motions present at temperatures above the transition may be important in biological function [6,10–13]. Several models have been used to describe the dynamics activated at the dynamical transition, including continuous diffusion [14], jumping between minima [3,5,15–17], mode-coupling theory [18–20], stretched-exponential behavior [21], and ''effective force constants'' [22]. Although these models are sometimes qualitatively different all can reproduce available experimental data well.

Even for relatively simple systems, distinguishing experimentally between microscopic dynamical models is possible only if the range of (Q,ω) accessed is large enough, including comprehensive quasielastic scattering measurements out to high enough values of Q and ω. However, neutron scattering is limited by counting statistics, and the intensity of the high Q and ω quasielastic scattering is often not high enough to permit its accurate determination. Often, the interpretation must be based on elastic scattering. To a first approximation the elastic scattering is proportional to $\exp[-(1/6)Q^2\langle\Delta r^2\rangle]$. It is therefore of particularly high intensity for atoms confined to microscopic volumes and at low Q. In such cases, it can be accurately measured and used to obtain a first estimate of the dynamics in the system. However, the elastic scattering does not necessarily contain sufficient information to distinguish between dynamical models. If this is is the case, questions must be raised which analytical model should be used in any given case and how physically meaningful derived quantities are, such as diffusion lengths, energy barriers, or effective force constants.

*Electronic address: biocomputing@iwr.uni-heidelberg.de

Here, we alleviate the problems associated with data overinterpretation by examining how one can extract useful information from experimental elastic incoherent neutron scattering data that goes beyond a simple determination of the mean-square displacement but without assuming a specific dynamical model. It was considered of particular importance in the present work to derive a way of treating the data that could be of practical use. To do this, we propose a method using a framework common to many analytical descriptions. The method proceeds in two stages: fitting to the Q dependence of the elastic scattering, followed by decomposition of the resulting $\langle \Delta r^2 \rangle$.

In the Q dependence analysis the importance of higher-order, non-Gaussian terms is underlined. Non-Gaussian behavior can have two origins. One is non-Gaussian dynamics of single atoms, an effect that has been extensively characterized previously [23]. The second effect, which can be particularly important in dynamically heterogeneous systems, arises from the existence of a distribution of mean-square displacements. It is shown here that, when this effect dominates, analysis of the Q dependence leads to the determination of the variance of the mean-square displacement.

In the second stage of the method contributions to the experimentally determined $\langle \Delta r^2 \rangle$ are analyzed. A formalism is presented in which the experimental $\langle \Delta r^2 \rangle$ consists of two parts: a converged (long time) part resulting from molecular vibrations and changes in the elastic incoherent scattering function (EISF), and a second contribution containing those displacements that are too slow to be resolved by the instrument used.

In Sec. III the method is applied to experimental data obtained on the temperature-dependence of the dynamics of a protein solution (Ref. [24]). The analysis leads naturally to the discussion of alternative mechanisms for the observed temperature dependence of the mean-square displacement, and it is shown that the data can be interpreted without requiring changes in the EISF.

The method for interpreting neutron scattering results proposed here is expected to be useful for interpreting the elastic incoherent scattering from a wide range of complex molecular systems.

II. THEORY

A. The dynamic structure factor

The basic quantity measured in incoherent neutron scattering experiment is the double-differential cross section, $\partial^2\sigma/\partial\Omega\,\partial E$, which is the number of neutrons incoherently scattered into the solid angle interval $[\Omega,\Omega+\Delta\Omega]$ with an energy transfer interval $[E,E+\Delta E]$. The dynamic structure factor is related to this cross section via

$$\frac{\partial^2\sigma}{\partial\Omega\,\partial\omega} = N\frac{k}{k_0}\sigma_0 S(\vec{Q},\omega), \tag{1}$$

where $E=\hbar\omega$, N denotes the number of atoms, k and k_0 the moduli of the incident and scattered wave vector, σ_0 is the incoherent scattering length of the atoms. For simplicity in writing in what follows this is assumed here to be the same for each atom. This is a reasonable assumption for hydrogen-rich samples for which the incoherent scattering cross section of hydrogen dominates the measured signal. However, the general case is easily obtained by summing contributions of the different isotopic species.

$S(\vec{Q},\omega)$ is expressed in terms of the intermediate scattering function $I(\vec{Q},t)$ and the van Hove autocorrelation function $G(\vec{r},t)$:

$$S(\vec{Q},\omega) = \frac{1}{2\pi}\int dt\; e^{-i\omega t} I(\vec{Q},t), \tag{2}$$

$$I(\vec{Q},t) = \frac{1}{2\pi}\int d\vec{r} e^{-i\vec{Q}\vec{r}} G(\vec{r},t), \tag{3}$$

$$G(\vec{r},t) = \frac{1}{N}\sum_i \int d\vec{r}' \langle \delta(\vec{r}-\vec{r}'+\vec{R}_i(0))\delta(\vec{r}'-\vec{R}_i(t))\rangle. \tag{4}$$

In Eqs. (2)–(4) $\vec{R}_i(t)$ is the position vector of atom i ($i=1,\ldots,N$) at time t and the brackets $\langle\cdots\rangle$ indicate an ensemble average. $G(\vec{r},t)$ is the probability that a certain particle can be found at position $\vec{r}$ at time t, given that it was at the origin at $t=0$ (here and throughout the article only the classical limit of these functions is considered). $G(\vec{r},t)$ describes how a system deviates from a given starting configuration. It is therefore a description of relaxation processes.

B. Quasielastic and elastic scattering

Here, we repeat the standard formulation of quasielastic and elastic neutron scattering that is commonly used as a starting point for analytical interpretation of experimental results. This formalism uses approximations that are sufficiently mild that they are likely to encompass the dynamics of most experimental scattering systems. The results of this section are discussed in detail in Ref. [1].

The common starting point for analyzing experimental spectra is to decompose the intermediate scattering function $I(\vec{Q},t)$ into a vibrational and diffusive part as follows:

$$I(\vec{Q},t) = I^V(\vec{Q},t)\cdot I^D(\vec{Q},t). \tag{5}$$

The vibrational part $I^V(\vec{Q},t)$ describes intramolcular and intermolecular vibrations of the system, whereas the diffusive part contains relaxation processes.

$S(\vec{Q},\omega)$ then reads

$$S(\vec{Q},\omega) = S^V(\vec{Q},\omega)\otimes S^D(\vec{Q},\omega). \tag{6}$$

The vibrational part can be written as

$$S^V(\vec{Q},\omega) = e^{-2W}\delta(\omega) + S^V_{inel}(\vec{Q},\omega), \tag{7}$$

where W is the Debye-Waller factor and $S^V_{inel}(\vec{Q},\omega)$ is inelastic scattering, consisting of peaks centered at the vibrational frequencies of the system and multiples thereof.

$S^D(\vec{Q},\omega)$ gives rise to the quasielastic part of the spectrum. For a spatially confined system it is typically given by a sum of Lorentzian functions as follows:

$$S^D(\vec{Q},\omega)=A_0(\vec{Q})\,\delta(\omega)+\sum_l A_l(\vec{Q})\cdot L_l(\lambda_l,\omega), \qquad (8)$$

where $A_0(\vec{Q})$ is the EISF and $L_l(\lambda_l,\omega)=(1/\pi)(\lambda_l/\lambda_l^2+\omega^2)$ is a Lorentzian of width λ_l.

The relaxation of the system is here decomposed into a sum of independent processes each labeled with the integer *l*. For certain dynamical models such as jump models, each of these processes can be assigned a physical meaning. For jump models the number of independent relaxation processes is given by the number of potential wells and each λ_l is given by a suitable combination of jump rates between minima (see Ref. [1] for details). Other dynamical models, such as diffusion-in-a-sphere, also lead to a sum of Lorentzians but lack a concrete physical interpretation of any single relaxation frequency λ_l.

Since we restrict our analysis to elastic scattering we neglect the inelastic scattering and write for the elastic and quasielastic scattering function

$$S(\vec{Q},\omega)=e^{-2W}\left(A_0(\vec{Q})\,\delta(\omega)+\sum_l A_l(\vec{Q})\cdot L_l(\lambda_l,\omega)\right). \qquad (9)$$

Equation (9) has been the starting point for the analysis of many quasielastic neutron scattering experiments on molecules. It has a form common to a wide class of microscopic models, including, for example, bounded diffusion or jump models. These models are commonly used to explain condensed-phase molecular scattering (see, e.g., [3,5,14–17]).

The form of the functions $A_0(\vec{Q})$ and $A_l(\vec{Q})$ depends on the analytical dynamical model used. If the system is sufficiently simple that the underlying dynamical process is qualitatively known then the forms of $A_0(\vec{Q})$ and $A_l(\vec{Q})$ can be analytically incorporated into the analysis of experimental elastic scattering data. For more complex systems, however, the functional form of the quasielastic scattering is not known *a priori*.

In what follows, we avoid having to elucidate $A_0(\vec{Q})$ and $A_l(\vec{Q})$ and hence avoid specifying the dynamical models associated with them, and examine data rather in a practical way, incorporating basic effects such as instrumental resolution and heterogeneity in the mean-square displacements.

C. *Q* dependence of $S(Q,0)$

We first consider the *Q* dependence of the elastic scattering. In what follows *Q* is spherically averaged so as to further mimic experimental conditions. For $Q\to 0$ the elastic scattering can be written as follows:

$$S(Q,0)=e^{-(1/6)Q^2\langle\Delta r^2\rangle}. \qquad (10)$$

This is often referred to as the ''Gaussian approximation'' [23]. The Gaussian approximation is strictly valid only in the limit $Q\to 0$ and experimental scattering in condensed-phase systems often exhibits non-Gaussian behavior.

There are two possible reasons for non-Gaussian behavior. First, the dynamics of single atoms may lead to non-Gaussian scattering and second, non-Gaussian behavior may arise due to a distribution of mean-square displacements in the molecular system. We call the latter ''dynamical heterogeneity.'' We now examine both of these two possibilities.

1. Non-Gaussian single-atom scattering

Non-Gaussian behavior can arise when the dynamics of single atoms exhibits certain properties. This case was treated in Ref. [23] and is only briefly summarized here. $I(Q,t)$ can be written as

$$I(Q,t)=\exp\left[-\sum_{l=1}^{\infty}(Q^2)^l\gamma_l(t)\right], \qquad (11)$$

where the $\gamma_l(t)$ are defined by *l*-point velocity correlation functions. In Ref. [23], it is shown that if $\gamma_l(t)\to C_l$ rapidly enough with time then the elastic scattering can be written as

$$S(Q,0)=\exp\left[-\sum_{l=1}^{\infty}(Q^2)^l C_l\right]. \qquad (12)$$

Comparison with the Gaussian approximation shows that the first constant is given by $C_1=\langle\Delta r^2\rangle/6$.

The right-hand side (RHS) of Eq. (12) can be expanded as

$$S(Q,0)=\exp\left[-\sum_l (Q^2)^l C_l\right]$$
$$=e^{-(1/6)Q^2\langle\Delta r^2\rangle}\left(1+\sum_{m=2}^{\infty} b_m(-Q^2)^m\right). \qquad (13)$$

The parameters b_m are combinations of the C_l, (e.g., $b_2=C_2$) and are, therefore, determined by the dynamics of the system.

2. Dynamical heterogeneity

Dynamical heterogeneity, i.e., a distribution of mean-square displacements, also leads to corrections to the Gaussian approximation. Assuming Gaussian single-atom scattering the elastic scattering function then reads

$$S(Q,0)=\frac{1}{N}\sum_i^N e^{-(1/6)Q^2\langle\Delta r_i^2\rangle}, \qquad (14)$$

where *i* denotes atoms $i=1,\ldots,N$. As a sum of Gaussians is not, in general, Gaussian, corrections to Eq. (10) result.

Formally, we can rewrite Eq. (14) as follows:

$$S(Q,0)=e^{-(1/6)Q^2\langle\Delta r^2\rangle}\left(\frac{1}{N}\sum_i^N e^{-(1/6)Q^2(\langle\Delta r_i^2\rangle-\langle\Delta r^2\rangle)}\right) \tag{15}$$

$$=e^{-(1/6)Q^2\langle\Delta r^2\rangle}\left[\sum_{m=0}^{\infty}\frac{1}{m!}\left(\frac{-Q^2}{6}\right)^m\mu(m)\right] \tag{16}$$

$$\approx e^{-(1/6)Q^2\langle\Delta r^2\rangle}\left(1+\frac{Q^4}{72}\sigma^2\right). \tag{17}$$

Here, $\langle\Delta r^2\rangle$ is the average mean-square displacement of the system, $\mu(m)$ is the mth central moment of the distribution of $\langle\Delta r^2\rangle$, and σ^2 is the variance. Eq. (17) is valid if $(-Q^2/6)^m\mu(m)\ll 1$. Thus, in systems where heterogeneity is the dominating contribution to non-Gaussian behavior, the elastic scattering can in principle be used to obtain experimentally the variance and higher statistical moments of the distribution of mean-square displacements.

3. Practical analysis of $S(Q,0)$

To incorporate non-Gaussian behavior without restricting the interpretation to a specific model, we propose the use of a heuristic function of the form

$$S(Q,0)=e^{-(1/6)Q^2\langle\Delta r^2\rangle}\left(1+\sum_{m=2}^{\infty}b_m(-Q^2)^m\right) \tag{18}$$

$$\approx e^{-(1/6)Q^2\langle\Delta r^2\rangle}(1+bQ^4). \tag{19}$$

Here, the b_m are parameters used to reproduce the experimentally observed elastic incoherent scattering. We showed in the preceding two sections that both aspects of non-Gaussian behavior, single-atom dynamics and heterogeneity, lead to a function of the form of Eq. (18). To what extent each of these effects contributes to non-Gaussian behavior will vary from system to system and is not known *a priori*. Therefore, using Eq. (18) and treating b_m as heuristic parameters is equivalent to making minimal assumptions about the system. In the low Q range, as long as deviations from Gaussian behavior are small, i.e., $b_m(Q^2)^m\ll 1$, we can neglect higher-order terms and can derive two parameters from the elastic scattering, $\langle\Delta r^2\rangle$ and b.

In the following section, the experimentally derived $\langle\Delta r^2\rangle$ thus obtained will be examined in detail.

D. Finite energy resolution and the mean-square displacement

Fitting experimentally obtained elastic scattering data using Eq. (18) [or Eq. (19) for small Q] yields the ''measured'' mean-square displacement, which we call $\langle\Delta r^2\rangle_{Expt}$. For any given instrument $\langle\Delta r^2\rangle_{Expt}$ may not be the time-converged mean-square displacement, but may have contributions due to finite energy resolution. We will now analyze the components of $\langle\Delta r^2\rangle_{Expt}$ using Eq. (9) as a starting point.

Inspection of Eq. (9) suggests that the elastic scattering can be obtained by neglecting the quasielastic term, $\Sigma_l A_l(\vec{Q})\cdot L_l(\lambda_l,\omega)$. However, in a real experiment due to finite energy resolution the intensity under the elastic peak can contain contributions from quasielastic scattering. To represent this analytically, we write the measured elastic scattering, $S_{Expt}(Q,0)$ as

$$S_{Expt}(Q,0)=\int d\omega R(\omega)S(Q,\omega) \tag{20}$$

$$=e^{-2W}\left(A_0(Q)+\sum_l A_l(Q)\Delta\omega_l\right), \tag{21}$$

where $R(\omega)$ is the instrumental energy resolution function and $\Delta\omega_l=\int d\omega R(\omega)L_l(\lambda_l,\omega)$.

Experimentally, $\langle\Delta r^2\rangle_{Expt}$ is obtained by plotting $\ln[S_{Expt}(Q,0)]$ against Q^2. Using the Gaussian approximation, we have

$$\langle\Delta r^2\rangle_{Expt}=-6\frac{\partial}{\partial Q^2}\ln[S_{Expt}(Q,0)]|_{Q^2=0}. \tag{22}$$

We thus obtain from Eq. (21) for the measured mean-square displacement

$$\langle\Delta r^2\rangle_{Expt}=-6\frac{\partial}{\partial Q^2}\ln[S_{Expt}(Q,0)]|_{Q^2=0} \tag{23}$$

$$=-6\frac{\partial}{\partial Q^2}\ln(e^{-2W}) \tag{24}$$

$$-6\frac{\partial}{\partial Q^2}\left(\ln\left[A_0(Q)+\sum_l A_l(Q)\Delta\omega_l\right]\right), \tag{25}$$

$$\langle\Delta r^2\rangle_{Expt}=\langle\Delta r^2\rangle_{Vib}+\langle\Delta r^2\rangle_{EISF}-\langle\Delta r^2\rangle_{Res} \tag{26}$$

$$=\langle\Delta r^2\rangle_{Conv}-\langle\Delta r^2\rangle_{Res}. \tag{27}$$

$\langle\Delta r^2\rangle_{Expt}$ in Eq. (27) contains two contributions. One of these, $\langle\Delta r^2\rangle_{Conv}$, is the long time, converged $\langle\Delta r^2\rangle$, consisting of the vibrational contribution $\langle\Delta r^2\rangle_{Vib}$, and the diffusive contribution associated with the EISF, $\langle\Delta r^2\rangle_{EISF}$.

The second term in Eq. (27), $\langle\Delta r^2\rangle_{Res}$ is the contribution to $\langle\Delta r^2\rangle_{EISF}$ due to relaxation processes too slow to be resolved by the instrument. Its negative sign means that it reduces the observed $\langle\Delta r^2\rangle$. Neglecting this second term corresponds to making the assumption that all motions in the system are fast enough to be detected.

$\langle\Delta r^2\rangle_{Res}$ is given by $\langle\Delta r^2\rangle_{Res}\equiv\Sigma_l a_l\Delta\omega_l$

with

$$a_l=6\frac{\partial}{\partial Q^2}A_l(Q)|_{Q^2=0}. \tag{28}$$

$\Delta\omega_l$, the width of the Lorentzian function, is assumed here to be independent of Q. This is true for most analytical models of spatially confined systems (e.g., jumping between

a finite number of states, rotational or confined diffusion). However, in heuristic approaches to experimental data treatment the width is often taken to be Q dependent, in which case $\langle \Delta r^2 \rangle_{Res}$ would contain a second term. This would, however, have no practical effect on the present analysis.

Noting that

$$\int_{-\infty}^{\infty} d\omega \frac{1}{\pi} \frac{\lambda_l}{\lambda_l^2 + \omega^2} = 1, \tag{29}$$

inspection of Eq. (26) shows that the maximal contribution of the relaxation mode $A_l(Q)$ to $\langle \Delta r^2 \rangle_{Res}$ is given by a_l. This is intuitive for systems in which a real physical process can be related to a given relaxation mode l. If a certain mode l describes, for example, jumping between two minima, this maximal contribution a_l is given by the distance between these minima, and Eq. (27) is simply the statement that these jumps will be detected only if they occur on time scales accessible to the instrument. However, for models where the physical process involved cannot be described by a single relaxation mode, no direct physical interpretation of a_l is possible.

Finally, we derive an approximate functional form of $\Delta\omega_l$. To do this, we make an approximation to the resolution function $R(\omega)$ that allows $\Delta\omega_l$ to be expressed analytically, i.e., $R(\omega)$ is assumed to be a rectangular function of width $\Delta\omega$,

$$R(\omega) = \begin{cases} 1, & -\Delta\omega \leqslant \omega \leqslant \Delta\omega \\ 0, & \text{other.} \end{cases} \tag{30}$$

This allows us to write

$$\langle \Delta r^2 \rangle_{Expt} = \langle \Delta r^2 \rangle_{Conv} - \sum_l a_l \frac{2}{\pi} \arctan \frac{\Delta\omega}{\lambda_l}. \tag{31}$$

Equation (31) provides the second equation of practical use in analyzing experimental data, the first being Eq. (18).

E. Finite energy resolution and dynamical heterogeneity

We now examine how the interpretation of the parameters of Eq. (17) changes if finite instrumental energy resolution is taken into account. The calculations are cumbersome so we restrict the analysis to the first correction b. From Eq. (17) it follows that

$$S_{Expt}(Q,0) = e^{-(1/6)Q^2\langle \Delta r^2 \rangle_{Expt}} + bQ^4 + O(Q^6), \tag{32}$$

where $O(Q^6)$ stands for terms of order Q^6 and higher. Thus, the correction term b can be calculated by expanding $[S_{Expt}(Q,0) - e^{-(1/6)}Q^2\langle \Delta r^2 \rangle_{Expt}]$ to fourth order in Q. This gives

$$bQ^4 = [S_{Expt}(Q,0) - e^{-(1/6)Q^2\langle \Delta r^2 \rangle_{Expt}}] = \frac{Q^4}{72}\sigma + O(Q^6). \tag{33}$$

Equation (26) gives

$$\langle \Delta r^2 \rangle_{Expt} = \langle \Delta r^2 \rangle_{Vib} + \langle \Delta r^2 \rangle_{EISF} - \sum_l a_l \Delta\omega_l, \tag{34}$$

where $\langle \Delta r^2 \rangle_{Vib}$ and $\langle \Delta r^2 \rangle_{EISF}$ make up the time-converged part and $-\Sigma_l a_l \Delta\omega_l$ is the contribution due to finite energy resolution.

Therefore,

$$\sigma = \sigma_{Vib} + \frac{1}{N}\sum_i^N \langle \Delta r_i^2 \rangle_{EISF}^2 - \sum_l a_{2_l} \Delta\omega_l - \left(\frac{1}{N}\sum_i^N \langle \Delta r_i^2 \rangle_{EISF} - \sum_l a_l \Delta\omega_l \right)^2, \tag{35}$$

where σ_{Vib}^2 is the variance of the vibrational $\langle \Delta r^2 \rangle_{Vib}$ and a_{2_l} is a multiple of the fourth-order coefficient of the Taylor expansion of $A_l(Q)$.

Inspection of Eqs. (35) and (34) show that in the case of perfect energy resolution, $\Delta\omega_l = 0$, Eq. (17) is recovered. Therefore, although finite energy resolution does not alter the form of Eq. (17), it does alter the interpretation of the obtained parameters, $\langle \Delta r^2 \rangle$ and σ.

F. Practical implementation

To conclude this section, we propose a protocol for using Eqs. (18) and (31) to analyze experimental data.

In a first step Eq. (18) is fitted to the Q dependence of the elastic scattering. The accessible Q range here determines how many independent parameters b_m should be incorporated in the analysis. For the example analyzed in Sec. III (in the range $Q^2 \leqslant 2$ Å^2), $\langle \Delta r^2 \rangle_{Expt}$ and one b parameter could be determined.

In the second step the obtained $\langle \Delta r^2 \rangle_{Expt}$ is further analyzed with Eq. (31). In practice, it is necessary to restrict the number of relaxation frequencies λ_l used—in the given example only one frequency, λ, was required, i.e.,

$$\langle \Delta r^2 \rangle_{Expt} = \langle \Delta r^2 \rangle_{Conv} - a \frac{2}{\pi} \arctan \frac{\Delta\omega}{\lambda}. \tag{36}$$

In what follows, we examine data on the temperature dependence of the scattering of a protein solution. Different hypotheses can be tested using Eq. (36). All fits were performed using a Marquardt-Levenberg algorithm as implemented in the Gnuplot program [25].

III. RESULTS

In this section, we use the formalism developed above to interpret a set of experimental data on the temperature dependence of the dynamics of a cryosolution of the protein glutamate dehydrogenase [24]. The data were obtained using the instrument IN6 at the Institut Laue-Langevin, with an energy resolution of ~ 50 μeV.

A. $S(Q,0)$ at low Q

Figure 1 shows fits of Eq. (19) to $\ln S(Q,0)$ versus Q^2 data

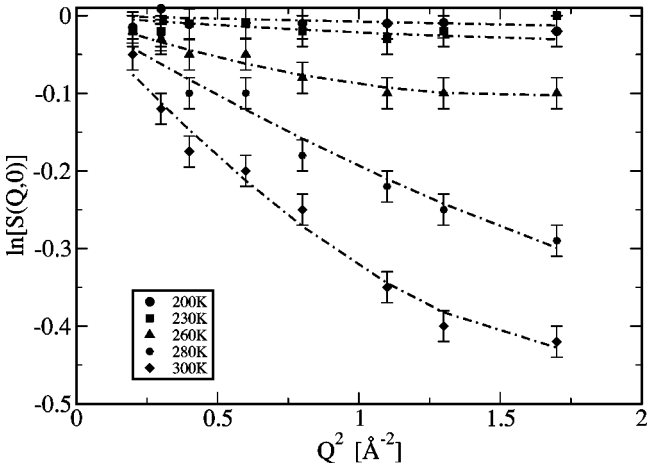

FIG. 1. Equation (17) (dot-dashed line) fitted to experimental data from Ref. [24].

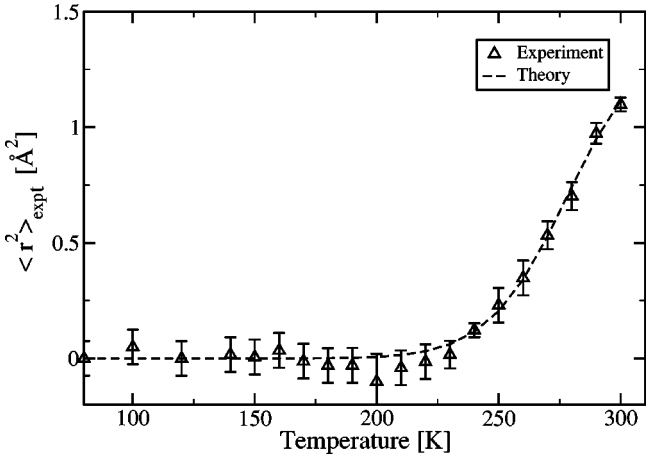

FIG. 2. $\langle \Delta r^2 \rangle_{Expt}$ determined on a protein solution (glutamate dehydrogenase in 70% CD_3OD/30% D_2O) using the instrument IN6 at the ILL [24], and fitted using Eq. (36).

at five different temperatures, following the procedure described in ''methods.'' The fits show that the data can be adequately fitted with terms up to $O(Q^4)$. The resulting parameters are shown in Table I. For a protein computer simulations have shown that over the Q range examined here ($0 \leqslant Q^2 \leqslant 2$ Å^2) the single-atom scattering is Gaussian and that non-Gaussian contributions arise principally from dynamical heterogeneity [26]. Thus, the parameters b can be assigned as σ, the variance of the mean-square displacement.

Some caution must be taken in interpreting the absolute values of the fitted parameters. Incorporating higher orders in Q, [up to $O(Q^8)$], while keeping initial values near those in Table I changed neither the value of the parameters $\langle \Delta r^2 \rangle$ and b, nor the goodness of fit. Therefore, the fit was locally stable. However, incorporating higher-order corrections and arbitrarily changing the initial values was found to lead to additional solutions with different absolute values of $\langle \Delta r^2 \rangle$ and b (data not shown). Nevertheless, all fits showed an increase in both $\langle \Delta r^2 \rangle_{Expt}$ and b going through the dynamical transition from low to high temperature.

The fact that fitting Eq. (19) is not stable against arbitrary changes of the initial values underlines the need to incorporate higher-order corrections even in the relatively low Q range ($0-2$ Å^{-2}) studied here. Clearly, however, the meaning of the corresponding coefficients will depend not only on the system dynamics but also on the accuracy of the experimental measurements—in some cases higher-order terms will compensate experimental errors.

TABLE I. Mean-square displacement and variance from fitting Eq. (17) to the experimental data obtained in Ref. [24].

T (K)	$\langle \Delta r^2 \rangle$ (Å^2)	b (Å^4)
200	0.02 ± 0.02	0.009 ± 0.009
230	0.08 ± 0.05	0.09 ± 0.09
260	0.37 ± 0.06	0.45 ± 0.1
280	0.6 ± 0.2	0.3 ± 0.2
300	1.1 ± 0.1	0.8 ± 0.1

B. Mean-square displacement

The next step is to interpret $\langle \Delta r^2 \rangle_{Expt}$ using the formalism outlined in Sec. II F. Figure 2 shows $\langle \Delta r^2 \rangle_{Expt}$ as a function of temperature. The data exhibit a dynamical transition at $\sim$220 K involving a sharp increase in $\langle \Delta r^2 \rangle_{Expt}$. Equation (31) shows that two different processes can lead to a temperature-dependent transition in $\langle \Delta r^2 \rangle_{Expt}$, a nonlinear change in $\langle \Delta r^2 \rangle_{EISF}$ with T or equally well a temperature dependence of the relaxation frequency λ. A discussion of both possibilities is now given.

1. Temperature-dependent $\langle \Delta r^2 \rangle_{EISF}$

Models involving a nonlinear temperature dependence of $\langle \Delta r^2 \rangle_{EISF}$ have been frequently invoked to explain dynamical transition behavior. We will therefore only briefly summarize them here. In these models, the dynamical transition results from a change with T of the equilibrium, converged, long-time atomic probability distribution, i.e., the EISF. One example of such models is that in Ref. [5] which consists of a two-state potential with a free-energy difference between the states of ΔU, separated by a distance d. The increased population of the higher energy state with increasing temperature leads to a transition in $\langle \Delta r^2 \rangle_{EISF}$ and, thus, $\langle \Delta r^2 \rangle_{Expt}$. Another model is that, in Refs. [22] and [27], in which the energy landscape is approximated by two harmonic potentials with different force constants. Here, the probability of atoms occupying the lower force-constant potential increases with temperature, thus, as well leading to an increase of $\langle \Delta r^2 \rangle_{EISF}$.

For the present purposes the distinguishing experimental characteristic of the above models is that they lead to $\langle \Delta r^2 \rangle_{Expt}$ independent of the instrumental resolution provided that resolution is sufficiently high that all the relaxation processes in the system are accessed.

2. Temperature-dependent $\langle \Delta r^2 \rangle_{Res}$

The alternative mechanism for nonlinear behavior of $\langle \Delta r^2 \rangle_{Expt}$ involves a nonlinear increase with T of $\langle \Delta r^2 \rangle_{Res}$,

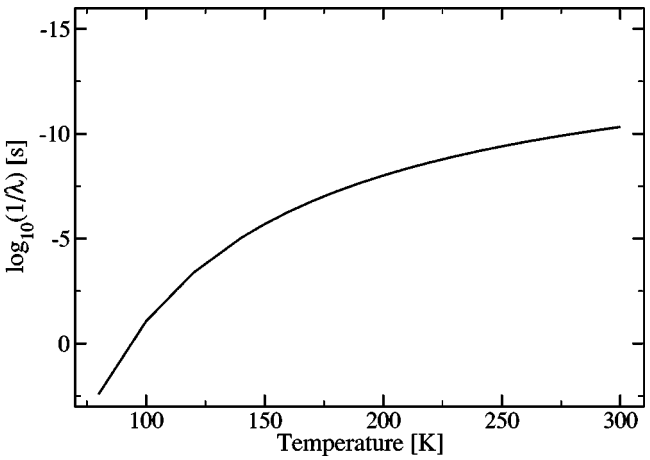

FIG. 3. Characteristic relaxation time $1/\lambda(T)$ as a function of temperature. $\lambda(T)$ was determined by fitting Eq. (31) to $\langle \Delta r^2 \rangle_{Expt}$ from Ref. [24].

due to motions becoming fast enough to be detected. In principle, this effect can lead to apparent dynamical transition behavior in the absence of any change in $\langle \Delta r^2 \rangle_{EISF}$. Figure 2 shows a fit of Eq. (36) to the experimentally determined $\langle \Delta r^2 \rangle$ from Ref. [24]. The agreement with experiment is satisfactory. Figure 3 shows the associated relaxation time $\tau(T)=1/\lambda(T)$. τ changes from the nanosecond to the picosecond time scale with increasing temperature, passing into the instrumental time resolution window of ~ 100 ps.

To understand the kind of physical process that can lead to a $\langle \Delta r^2 \rangle_{Res}$—driven apparent dynamical transition it is instructive to temporarily suspend our analysis and to consider a simple potential of the form illustrated in Fig. 4, in which two identical wells are separated by a barrier of height ΔU. Assuming jumping between the wells the scattering function of such a potential is well known and is as follows (see Ref. [28] for details):

$$S(Q,\omega)=\exp\left(-\frac{1}{2}Q^2\langle \Delta r^2 \rangle_{Vib}\right)\left[A_0(Q)\,\delta(\omega) + \frac{1}{\pi}A_1(Q)\,\frac{2\tau}{4+\omega^2\tau^2}\right], \tag{37}$$

with

$$A_0(Q)=\frac{1}{2}[1+j_0(Qd)],$$

$$A_1(Q)=\frac{1}{2}[1-j_0(Qd)],$$

with $j_0(x)$ being the zeroth-order Bessel function of the first kind, $1/\tau$ the jump rate and d the distance between the minima. The term $\exp(-\frac{1}{2}Q^2\langle \Delta r^2 \rangle_{Vib})$ is the Debye-Waller factor due to vibrational motions not included in the jump model.

The probability of finding a particle in one of the two wells is $\frac{1}{2}$ and is independent of temperature. Consequently,

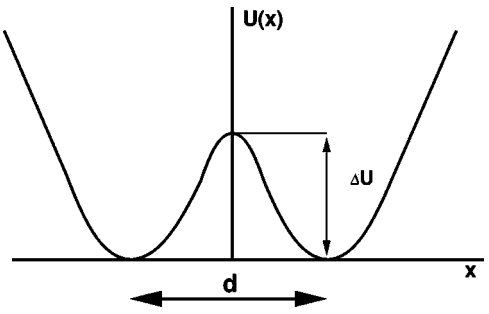

FIG. 4. Double-well potential.

there will be no change in $\langle \Delta r^2 \rangle_{EISF}$ with temperature. However, an apparent dynamical transition can occur through finite energy resolution effects.

Using Eq. (37) as starting point and repeating the steps leading from Eq. (9) to Eq. (31) $\langle \Delta r^2 \rangle_{Expt}$ reads

$$\langle \Delta r^2 \rangle_{Expt}=\langle \Delta r^2 \rangle_{Vib}+\frac{6d^2}{4}\left[\frac{1}{2}-\frac{1}{\pi}\arctan\left(\frac{\Delta\omega}{2}\tau\right)\right]. \tag{38}$$

With $\langle \Delta r^2 \rangle_{EISF}=6d^2/8, a=6d^2/8$, and $\lambda=1/\tau$ this is of the form of Eq. (36).

A suitable functional form of $\tau(T)$ for barrier crossing is Arrhenius: $\tau(T)=ae^{b/T}$. For the potential of Fig. 4 the parameter b is related to the energy by $b=\Delta U/k$, k being the Boltzmann constant. The parameters then resulting from the fit in Fig. 2 are shown in Table II. However, as we have discussed, this interpretation is model dependent and, as we have discussed, these parameters may not be physically realistic. Describing the transition by Eq. (36) is more general than assuming a specific model, and is equally valid for a model based, for example, on diffusion in a sphere, in which case λ would be related to a diffusion constant and b not directly related to an energy barrier. Figure 3 retains generality in that any dynamical model fulfilling the assumptions leading to Eq. (36) and having a temperature dependence of the relaxation frequency similar to Fig. 3 will lead to the same observed transition behavior.

In this section, we showed how the formalism derived in Sec. II can be used to analyze experimentally obtained elastic incoherent scattering spectra. Eqs. (19) and (36) are suitable functions that can be used to test hypotheses concerning experimental phenomena such as the dynamical transition. Different interpretations are consistent with experimental mean-square displacements observed for a protein solution, thus, stressing the necessity of an analysis of experimental scatter-

TABLE II. Parameters obtained by analyzing $\langle \Delta r^2 \rangle_{Expt}$ in terms of a double-well potential (see Fig. 4).

	$\langle \Delta r^2 \rangle_v / T$ $\left(\frac{\text{Å}^2}{\text{K}}\right)$	ΔU $\left(\frac{\text{kcal}}{\text{mol}}\right)$	d (Å)	τ_0 (s)
IN6	0.0003	5.3 ± 0.2	1.4 ± 0.1	$1.1\cdot10^{-15}$

ing for complex molecular systems that encompasses a wide range of dynamical phenomena.

IV. SUMMARY

This paper presents a method of analyzing elastic incoherent neutron scattering of dynamically heterogeneous molecular systems in which the form of the energy landscape is not imposed. The need for this approach has arisen from the realization that, for complex systems that may possess a variety of anharmonic dynamics, the imposition of a simplified analytical model (e.g., a double well or spherical potential) may be over-restrictive.

The present analysis concentrates on elastic incoherent scattering and explicitly incorporates effects of the instrumental energy resolution. In doing so a practical analysis method is proposed that should be of widespread applicability. The method consists of two separate steps. In the first step the measured elastic scattering spectra is fitted to Eq. (18). This function incorporates non-Gaussian behavior. Non-Gaussian elastic scattering arises either from non-Gaussian single-atom dynamics of the system or by heterogeneity of the mean-square displacements. Both effects lead to corrections of the order Q^4.

In a second step the obtained parameters are further analyzed. Equation (31) describes the experimentally determined mean-square displacement, $\langle \Delta r^2 \rangle_{Expt}$ in terms of a converged displacement, $\langle \Delta r^2 \rangle_{Conv}$ that would be obtained with an instrument of perfect energy resolution, and a contribution due to unresolved motions present in the system described by λ, a relaxation frequency and a, the amount this relaxation mode contributes to $\langle \Delta r^2 \rangle_{EISF}$.

The description of the $\langle \Delta r^2 \rangle$ in terms of converged and resolution-dependent contributions highlights two possible causes of dynamical transition behavior in condensed-phase systems. One of these describes the transition in terms of a change in the (long-time) equilibrium position distribution leading to a nonlinear increase in $\langle \Delta r^2 \rangle_{EISF}$. The temperature at which this occurs is independent of the instrumental energy resolution. In the alternative mechanism the temperature dependence of the dynamical relaxation frequency, λ leads to acceleration of the relaxation processes with increasing temperature until they become detectable by the instrument. This leads to an apparent dynamical transition originating in the variation of $\langle \Delta r^2 \rangle_{Res}$ with the instrumental energy resolution. It is demonstrated here that this alternative description can reproduce experimental data for a protein solution, obtained in Ref. [24]. However, in many systems, including protein solutions, the complexity of the energy landscape may lead to both kinds of transitions occurring. Therefore, in these cases the relevant problem would not be the determination of which of the two alternative descriptions of the dynamical transition is present, but rather separation of the contributions of both. This separation requires extraction of the EISF from incoherent scattering measurements. For this it is necessary to accurately determine the temperature dependence of both the quasielastic and elastic contributions and to characterize the relaxation processes in more detail by analyzing $S(Q,\omega)$ and $I(Q,t)$.

[1] M. Bee, *Quasielastic Neutron Scattering: Principles and Applications in Solid-state Chemistry, Biology and Materials Science* (Hilger, Bristol, 1988).

[2] S. Lovesey *Theory of Neutron Scattering from Condensed Matter* (Oxford University Press, New York, 1987), Vol. 1.

[3] H. Frauenfelder, G.A. Petsko, and D. Tsernoglou, Nature (London) **280**, 558 (1979).

[4] H. Keller and P.G. Debrunner, Phys. Rev. Lett. **45**, 68 (1980).

[5] W. Doster, S. Cusack, and W. Petry, Nature (London) **337**, 754 (1989).

[6] B.F. Rassmussen, A.M. Stock, D. Ringe, and G.A. Petsko, Nature (London) **357**, 523 (1992).

[7] S.G. Cohen, E.R. Bauminger, I. Nowik, S. Ofer, and J. Yariv, Phys. Rev. Lett. **46**, 1244 (1981).

[8] A.R. Bizzarri, A. Paciaroni, and S. Cannistraro, Phys. Rev. E **62**, 3991 (2000).

[9] E.W. Knapp, S.F. Fischer, and F. Parak, J. Phys. Chem. **86**, 5042 (1982).

[10] M. Ferrand, A.J. Dianoux, W. Petry, and G. Zaccai, Proc. Natl. Acad. Sci. U.S.A. **90**, 9668 (1993).

[11] J. Fitter, R.E. Lechner, and N.A. Dencher, Biophys. J. **73**, 2126 (1997).

[12] U. Lehnert, V. Reat, M. Weik, G. Zaccai, and C. Pfister, Biophys. J. **75**, 1945 (1998).

[13] X. Ding, B.F. Rasmussen, G.A. Petsko, and D. Ringe, Biochemistry **33**, 9285 (1994).

[14] G.R. Kneller and J.C. Smith, J. Mol. Biol. **242**, 181 (1994).

[15] R. Elber and M. Karplus, Science **235**, 318 (1987).

[16] A. Lamy, M. Souaille, and J.C. Smith, Biopolymers **39**, 471 (1996).

[17] H. Frauenfelder, S. Sligar, and P. Wolynes, Science **254**, 1598 (1991).

[18] W. Doster and M. Settles in *Hydration Processes in Biology*, Vol. 305 of *NATO Science Series: Life Sciences*, edited by M. -C. Bellisent-Funel and J. Teixera (IOS Press, Amsterdam, 1999).

[19] A. Perico and R. Pratolongo, Macromolecules **30**, 5958 (1997).

[20] G. La Penna, R. Pratolongo, and A. Perico, Macromolecules **32**, 506 (1999).

[21] S. Dellerue, A.-J. Petrescu, J.C. Smith, and M.-C. Belissent-Funel, Biophys. J. **81**, 1666 (2001).

[22] G. Zaccai, Science **288**, 1604 (2000).

[23] A. Rahman, K.S. Singwi, and A. Sjölander, Phys. Rev. **126**, 986 (1962).

[24] R.M. Daniel, J.C. Smith, M. Ferrand, S. Hery, R. Dunn, and J.L. Finney, Biophys. J. **75**, 2504 (1998).

[25] D.W. Marquardt, J. Soc. Ind. Appl. Math. **11**, 431 (1963).

[26] J. Hayward and J.C. Smith, Biophys. J. **82**, 1216 (2002).

[27] D.J. Bicout and G. Zaccai, Biophys. J. **80**, 1115 (2001).

[28] C.T. Chudley and R.J. Elliott, Proc. Phys. Soc. London **77**, 353 (1961).